https://doi.org/10.5194/essd-2025-242
Preprint. Discussion started: 10 July 2025

Open Access Earth System Science Data Discussions

A lacustrine surface-sediment pollen dataset covering the Tibetan Plateau and its potential in past vegetation and climate reconstructions

Fang Tian[1], Weiyu Cao[1], Xiaohan Liu[1], Zixin Liu[1], Xianyong Cao[2]

[1] *College of Resource Environment and Tourism, Capital Normal University, Beijing 100048, China*

[2] *Group of Alpine Paleoecology and Human Adaptation (ALPHA), State Key Laboratory of Tibetan Plateau Earth System, Environment and Resources (TPESER), Institute of Tibetan Plateau Research, Chinese Academy of Sciences, Beijing 100101, China*

Correspondence: Fang Tian (tianfang@cnu.edu.cn)

Abstract. A dataset of pollen extracted from the surface-sediments of lakes with an even spatial distribution is essential for pollen-based reconstructions of past vegetation and climate. We collected 90 lake surface-sediment samples from the Tibetan Plateau (TP) covering major vegetation types. A comprehensive modern pollen dataset is established by integrating our newly obtained modern pollen dataset with previous modern lacustrine pollen datasets, covering the full range of climatic gradients across the TP with mean annual precipitation (P_{ann}) from 97 to 788 mm, mean annual temperature (T_{ann}) -9.09 to 6.93 °C, mean temperature of the coldest month (Mt_{co}) -23.48 to -2.65°C, and mean temperature of the warmest month (Mt_{wa}) 1.77 to 19.26°C. Numerical analyses revealed that P_{ann} is the primary climatic determinant for pollen distribution, while net primary production (NPP) is a valuable variable reflecting vegetation conditions. To detect the quantitative relationship between pollen and P_{ann}/NPP, both weighted-averaging partial least squares (WA-PLS) and random forest algorithm (RF) were employed. The performance of both models suggests that this modern pollen dataset has good predictive power in estimating past NPP and P_{ann}, but RF has a slight advantage with this dataset. This comprehensive modern pollen dataset is considered reliable when reconstructing vegetation and climate from pollen spectra from the central TP, but caution is needed if it is applied to pollen spectra from the marginal regions of the TP and those covering the Last Glacial period, due to poor analogue quality in those cases. The dataset, including site locations, pollen percentages, NPP, and climate data for 90 lakes, is available at the National Tibetan Plateau Data Center (TPDC; Tian, 2025; https://doi.org/10.11888/Paleoenv.tpdc.302470).

https://doi.org/10.5194/essd-2025-242
Preprint. Discussion started: 10 July 2025

1 Introduction

A modern pollen dataset is the foundation for the quantitive reconstruction of past vegetation and climate based on fossil pollen spectra. Surface-soil samples for pollen analysis can be easily obtained, but their pollen assemblages are easily affected by local vegetation components, which cause more noise in the modern relationships of pollen–climate and pollen–vegetation (Cao et al., 2014). Sediment from lakes, in contrast, provide more regional pollen signals owing to broader pollen source areas, more stable sedimentation rates, and better preservation, making them more suitable for regional vegetation and climate changes (Tian et al., 2020; Cao et al., 2021). Due to the sparse distribution of lakes, high sampling costs, and limited accessibility—especially in remote regions—modern pollen datasets from lake surface sediments remain limited and spatially biased, particularly in China (Herzschuh et al., 2010; Ma et al., 2017; Cao et al., 2021).

Situated at high elevations and subject to complex climate systems, the Tibetan Plateau (TP) is highly sensitive to global climate change and human activities and exhibits strong regional ecological and climatic peculiarities (Chen et al., 2015, 2020; Pepin et al. 2019). These features make the TP a research hotspot for past climate and vegetation reconstructions. Fortunately, the widespread distribution of lakes across the plateau offers an opportunity to expand and refine pollen-based calibration datasets using lake surface sediments., but the distribution of available pollen datasets of lake surface-sediment remains uneven and incomplete due to logistical constraints (Cao et al., 2021; Qin, 2021; Ma et al., 2024). Hence, it is essential to improve the coverage and comprehensiveness of the modern calibration-set from lake surface-sediments on the TP.

Previous pollen–climate relationships are often the focus of calibration-set studies, while the pollen–vegetation relationship is also crucial on the TP, where vegetation type is generally employed as the target variable, especially when reconstructing ecological conditions (e.g. Qin, 2021, Qin et al., 2022). However, the available modern pollen datasets reveal that pollen assemblages from different vegetation types on the TP generally present only minor differences in pollen components and their abundance. For instance, the dominant pollen taxa are generally herbaceous taxa including Cyperaceae, *Artemisia*, Amaranthaceae (=Chenopodiaceae), and Poaceae (e.g. Herzschuh et al., 2010; Ma et al., 2017; Cao et al., 2014, 2021; Li et al., 2020; Qin, 2021), making it difficult to distinguish vegetation conditions based on pollen assemblages directly. Net primary production (NPP), which quantifies the amount of atmospheric carbon fixed by plants and accumulated as biomass, plays an important role in the global carbon cycle (Fang et al., 2001; Nemani et al., 2003; Gonsamo et al., 2013; Ni, 2013; Walker et al., 2015; Ji et al., 2020). Therefore, NPP may serve as a

https://doi.org/10.5194/essd-2025-242
Preprint. Discussion started: 10 July 2025

more sensitive alternative variable in reflecting the spatial distribution and temporal change of vegetation conditions on the TP.

Here, we analysed 90 lake surface-sediment samples for pollen and combined them with previously published modern pollen data extracted from lake surface-sediments (Herzschuh et al., 2010; Li and Li, 2015; Cao et al., 2021; Ma et al., 2024; Wu et al., 2024), then used a combination of ordination techniques, weighted averaging partial least squares (WA-PLS), and Random Forest (RF) to: (1) establish a comprehensive pollen dataset extracted from lake surface-sediments covering the entire TP with an even distribution; (2) evaluate the predictive power of models using the modern pollen dataset in reconstructing past climate and vegetation.

2 Study area

Climate of the TP is controlled mainly by the Asian Summer Monsoon in summer with warm-wet conditions and by westerlies in winter with a cold-dry climate (Wang, 2006). In addition, there is a gradient from high summer temperatures (up to 19°C) and high precipitation (>700 mm) on the south-eastern TP, to low summer temperatures (ca. 6°C) and low precipitation (<100 mm) on the north-western TP (Fig. 1; Sun, 1999; Herzschuh, 2007; He et al., 2020).

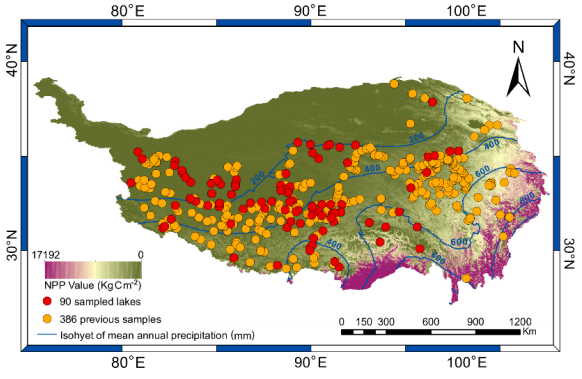

Figure 1. Spatial distribution of 476 modern pollen samples collected from lake surface-sediments on the Tibetan Plateau (red filled circles: 90 sampled lakes; orange filled circles: 386 previous samples, Herzschuh et al., 2010; Li and Li, 2015; Cao et al., 2021; Ma et al., 2024; Wu et al., 2024).

The TP exhibits distinct vegetation zonation along its south-east–north-west thermal and moisture gradients, progressing from forest ecosystems through alpine meadows and steppes to desert vegetation (Fig. 1; Zhang, 2007). Forests dominated by *Pinus*, *Picea*, *Abies*, *Betula*, *Quercus*, and *Tsuga* are primarily distributed in the warm-humid south-eastern and eastern marginal regions of the TP (Herzschuh, 2007). Alpine meadows, as one of the most important vegetation types, mainly distributed on the eastern and southern TP, and are characterized by *Kobresia* spp., *Carex*, Asteraceae,

https://doi.org/10.5194/essd-2025-242
Preprint. Discussion started: 10 July 2025

Polygonum, *Potentilla*, Fabaceae, Caryophyllaceae, *Leontopodium*, *Arenaria*, *Ranunculus,* and Poaceae (Wu, 1995; Herzschuh et al., 2010; Cao et al., 2021). Alpine steppes are primarily distributed across the southern, eastern, and central TP, and is mainly dominated by *Stipa purpurea*, *Artemisia*, *Potentilla*, Asteraceae, Amaranthaceae, and *Carex* (Fig. 1; Zhang, 2007; Yue et al., 2011). Alpine deserts, located in the dry north-central and westernmost central TP, are characterized by sparse vegetation, and are predominantly occupied by drought-tolerant taxa such as *Ceratoides* (Amaranthaceae), *Salsola*, *Haloxylon*, *Kalidium*, *Artemisia*, *Ephedra*, *Nitraria,* and Poaceae (Fig. 1; Zhang, 2007).

3 Materials and methods

3.1 Sample collection and pollen processing

To ensure the even distribution of the sampled lakes, we collected lake surface-sediment samples (the top 2 cm, n=90) from the centre of each lake in forest (n=5), meadow (n=22), steppe (n=53), and desert (n=10) vegetation types on the TP between 2021 and 2023 (Fig. 1, Table 1). The elevation range of these lakes varies from 3923 to 5433 m a.s.l. with a median of 4652 m a.s.l. (Fig. 1).

Table 1. Locations of the sampling sites of our field work on the Tibetan Plateau.

No.	Lake	Latitude (°N)	Longitude (°E)	Elevation (m a.s.l.)	Vegetation type
1	Cuomujiri	94.4304	29.8118	4235	Forest
2	Ranwu Lake	96.8252	29.3962	5263	Forest
3	Sanse Lake	94.7670	30.7239	4042	Forest
4	Ren Co	96.6748	30.7156	4452	Forest
5	Potal Lake	95.5743	31.6223	4656	Forest
6	Ruba Lake	90.1725	29.4644	3923	Meadow
7	Namucoluo	90.3347	29.6070	4690	Meadow
8	Cuoriwang	90.4064	30.0345	4400	Meadow
9	Niangde Co	90.1834	29.2810	4365	Meadow
10	Cona Lake	91.4305	32.0779	4602	Meadow
11	Tangbin Lake	90.9672	30.4795	5025	Meadow
12	Cuoe	91.5350	31.5088	4511	Meadow
13	Changma Lake	92.1069	32.0639	4932	Meadow
14	Cuomuri	92.0596	31.6201	4547	Meadow
15	Gemu Co	91.6990	31.5550	4524	Meadow
16	Xiongmu Co	91.6303	31.0399	4662	Meadow
17	Nairi Pingco	91.4788	31.2730	4513	Meadow
18	Cuomuzhelin	88.2168	28.3933	4395	Meadow
19	Nariyong Co	91.9377	28.3071	4731	Meadow
20	Peiku Co	85.5869	28.8507	4561	Meadow
21	Zhegu Co	91.6770	28.6316	4601	Meadow
22	Nianjie Co	96.2905	33.0773	4441	Meadow

https://doi.org/10.5194/essd-2025-242
Preprint. Discussion started: 10 July 2025

23	Samu Co	93.7813	30.9753	4748	Meadow
24	Haling Lake	97.5967	38.2507	4071	Meadow
25	Zhaling Lake	97.3420	34.9447	4280	Meadow
26	Koucha Lake	97.2311	34.0081	4518	Meadow
27	Eling Lake	97.7130	35.0217	4257	Meadow
28	Gelu Co	92.4546	34.5942	4639	Steppe
29	UlanUl Lake	90.7108	34.8528	4857	Steppe
30	Xijir Ulan Lake	90.3528	35.1875	4769	Steppe
31	Lexiewudan Lake	90.2053	35.7071	4862	Steppe
32	Xiangyang Lake	89.4616	35.8194	4843	Steppe
33	Kekexili Lake	91.2205	35.6115	4875	Steppe
34	Kekao Lake	91.3874	35.6973	4881	Steppe
35	Zhuonai Lake	91.9833	35.5325	4734	Steppe
36	Kusai Lake	92.9412	35.6753	4471	Steppe
37	Zigêtang Co	90.8973	32.0674	4538	Steppe
38	Daru Co	90.7324	31.6562	4675	Steppe
39	Bange Lake	89.4734	31.7282	4519	Steppe
40	Lingge Co	88.7220	33.9370	5061	Steppe
41	Qiagang Co	88.3966	33.2313	4719	Steppe
42	Caiduochaka Lake	88.9793	33.1576	4833	Steppe
43	Eya Co	88.6713	33.0013	4824	Steppe
44	Ri Co	89.6068	30.9302	4648	Steppe
45	Mujiu Co	89.0144	31.0337	4664	Steppe
46	Suo Co	90.9056	31.3978	4556	Steppe
47	Mading Co	90.2995	31.4147	4680	Steppe
48	Maiding Co	90.3202	31.8413	4773	Steppe
49	Changma Co	87.8756	32.2605	4725	Steppe
50	Cuolongjiao	88.8539	32.7857	4873	Steppe
51	Duomaxiang Lake	89.1268	32.3249	4704	Steppe
52	Gewa Co	88.7968	30.6725	4745	Steppe
53	Wojiong Co	89.3646	31.6276	4598	Steppe
54	Gaa Co	88.9583	32.2130	4602	Steppe
55	Chelachapuka	86.1548	31.8024	4773	Steppe
56	Yong Co	84.7044	31.9383	4712	Steppe
57	Rena Co	84.2559	32.7281	4579	Steppe
58	Chabo Co	84.2108	33.3512	4500	Steppe
59	Jibuchaga Co	83.9975	32.0205	4467	Steppe
60	Cuoguo Co	83.2921	32.2503	4669	Steppe
61	Bieruoze Co	82.9417	32.4308	4392	Steppe
62	Shekazhi	82.0466	32.0115	4591	Steppe
63	Dagze Co	87.4456	31.8332	4465	Steppe
64	Xiabie Co	87.2680	32.2179	4592	Steppe
65	Jiaruo Co	86.6001	32.1730	4445	Steppe
66	Xuguo Co	90.3251	31.9542	4598	Steppe

https://doi.org/10.5194/essd-2025-242
Preprint. Discussion started: 10 July 2025

67	Beilei Co	88.4296	32.9120	4797	Steppe
68	Unknown	81.7962	31.1937	5433	Steppe
69	Nading Co	85.4359	32.6776	4845	Steppe
70	Bala Co	82.9849	33.4281	4757	Steppe
71	Dong Co	84.7120	32.1440	4388	Steppe
72	Xiaogemu Co	85.7384	33.5778	4711	Steppe
73	Ningri Co	85.6752	33.3333	5020	Steppe
74	Guping Lake	85.6787	33.1683	5030	Steppe
75	Qiuruba Co	84.7966	33.3073	4733	Steppe
76	Caima'er Co	84.5879	33.5469	4573	Steppe
77	Selin Co	88.6979	31.7363	4512	Steppe
78	Zhari Namco	85.4004	30.9068	4595	Steppe
79	Kuhai Lake	99.1636	35.3070	4117	Steppe
80	Donggi Cona	98.6596	35.2875	4066	Steppe
81	Aru Co	82.4768	33.9682	4904	Desert
82	Aksai Chin Lake	79.7863	35.2456	4831	Desert
83	Kunchuke Co	82.6590	33.7096	5042	Desert
84	Xiawei Lake	82.0454	34.6738	5110	Desert
85	Luotuo Lake	81.9849	34.4339	5082	Desert
86	Meima Co	82.4404	34.1278	4897	Desert
87	Lhanag Co	81.2820	30.6674	4577	Desert
88	Hongshan Lake	80.0545	34.8300	5043	Desert
89	Manasarovar Lake	81.3939	30.7465	4577	Desert
90	Xiada Co	79.3584	33.3916	4338	Desert

For each sample, 2–3 g of dry material was used for pollen extraction, and a tablet with *Lycopodium* spores (10,315 grains) was added to each sample initially as tracers (Maher, 1981). Pollen samples were processed using standard acid–alkali–acid procedures (Fægri and Iversen, 1989), including 10% HCl, 10% KOH, 40% HF, acetolysis treatment, and sieving in an ultrasonic bath to remove particles <7 μm. Pollen grains were identified and counted under a Zeiss optical microscope at 400× magnification, referring to modern pollen slides collected from the eastern and central TP and published palynological literatures (Wang et al., 1995; Tang et al., 2016; Cao et al., 2020). To ensure the reliability of the pollen assemblages for numerical analyses, more than 500 terrestrial pollen grains, or over 2000 *Lycopodium* spores were counted for each sample. The pollen diagram was constructed using Tilia software (Grimm, 1987, 1991).

3.2 Data collection and harmonization

We compiled a dataset of modern pollen assemblages from lake surface sediments across the Tibetan Plateau, incorporating 375 lakes situated in eastern (Herzschuh et al., 2010; Cao et al., 2021), central, and western TP (Ma et al., 2024; Wu et al., 2024), obtained from accessible databases or from authors directly. To enhance spatial

https://doi.org/10.5194/essd-2025-242
Preprint. Discussion started: 10 July 2025

coverage, an additional 11 surface pollen assemblages were digitized from published diagram representing sites along the eastern edge of TP (Li and Li, 2015). The total dataset comprises 476 pollen assemblages from lake surface-sediments on the TP (Fig. A1).

The pollen data are standardized following the procedures outlined in Cao et al. (2013), including harmonization of taxonomy – generally to the family or genus level – and recalculation of pollen percentages based on total terrestrial pollen grains. Only pollen taxa with an abundance of at least 0.5% in at least three samples and a maximum ≥3% were retained for statistical analyses (n=35).

We employed the Chinese Meteorological Forcing Dataset (CMFD), a gridded near-surface meteorological dataset covering the period from January 1979 to December 2018, with a temporal resolution of 3 h and a spatial resolution of 0.1°. Climate data of each sampled lake were assigned as the values of the nearest pixel from the meteorological dataset. For each lake, the following parameters were extracted: P_{ann}: mean annual precipitation, mm; T_{ann}: mean annual temperature, °C; Mt_{co}: mean temperature of the coldest month, °C; Mt_{wa}: mean temperature of the warmest month, °C (He et al., 2020). The geographical distances between lake coordinates and grid centroids were calculated geodetically using the the *rdist.earth* function in the *fields* package version 16.3.1 for R (R Core Team, 2019; Nychka et al., 2025).

The NPP value, defined as Gross Primary Productivity (GPP) minus Maintenance Respiration (MR) (Zhao and Running, 2010), was obtained from observations of the MOD17A3HGF.006 product during 2001–2022 with a pixel resolution of 1000 m. Across the study region, NPP values range from 0.16 to 6617.36 Kg C m^{-2}, P_{ann} ranging from 97 to 788 mm, and cold thermal conditions characterized by low T_{ann} (-9.09 to 6.93°C) and Mt_{co} (-23.48 to -2.65°C; Table 2).

3.3 Data analysis

To visualize how the modern pollen assemblages respond to climatic variables, ordination techniques were employed. Pollen data were square-root transformed to stabilize variances and optimize the signal-to-noise ratio (Prentice, 1980). Detrended correspondence analysis (DCA; Hill and Gauch, 1980) showed that the gradient length of the first axis of the pollen data was 2.36 SD (standard deviation units), indicating that a linear response model is suitable for our pollen dataset (ter Braak and Verdonschot, 1995). We employed redundancy analysis (RDA) to assess how major pollen taxa and sampling sites are distributed along climate gradients. Climatic predictors were introduced sequentially following a forward selection procedure, with multicollinearity assessed at each step via variance inflation factors (VIF). Variables exhibiting VIF values above the threshold of 20 were excluded to maintain model parsimony and reduce redundancy (ter Braak and Prentice, 1988; Birks, 1995). Additionally, the suitability of each climatic variable for quantitative reconstruction was

https://doi.org/10.5194/essd-2025-242
Preprint. Discussion started: 10 July 2025

evaluated using the ratio of the first constrained eigenvalue to the first unconstrained eigenvalue (λ1/λ2), where larger ratios indicate stronger predictive potential (Juggins, 2013). All ordinations were carried out using the *rda* and *decorana* functions in the *vegan* package (Oksanen et al., 2019).

WA-PLS regression was applied to calibrate transfer functions linking modern pollen assemblages to Pann and NPP, based on square-root transformed relative abundances of the 35 selected taxa—consistent with those used in the ordination analyses (ter Braak and Juggins, 1993). Model performance was evaluated using "leave-one-out" cross-validation, and the optimal number of WA-PLS components were determined based on a randomization *t*-test (Juggins and Birks, 2012). All the analyses were performed using the *WA-PLS* function of the *rioja* package version 0.7–3 (Juggins, 2012) in R.

As WA-PLS is known to produce systematic prediction biases near the ends of environmental gradients—commonly referred to as the "edge effect" (Birks, 1998; Tian et al., 2022) —we further explored a complementary reconstruction method. Random Forest (RF) is an ensemble learning algorithm that integrates multiple decision trees based on a classification tree algorithm and summarizes their results for classification or regression tasks (Breiman, 2001). The importance of the explanatory variable is normally measured as a percentage increase in the residual sum of squares after random shuffling of the order of the variables, thereby determining which explanatory variable can be added to the model. RF has been applied in the geographical and ecological fields and performs well (Li, 2013; Jin et al., 2016). In this study, we applied RF to establish the importance of pollen and the NPP/climate variables (Table S1). The model was systematically optimized through a stepwise reduction procedure, in which the pollen taxa with the least important score was deleted until the RF-importance of all remaining taxa were greater than 0 (Breiman, 2001). The RF algorithm was run based on square-root transformed pollen percentages, using the *randomForest* function in the *randomForest* package version 4.6–14 (Liaw, 2018) in R. The statistical significance of the reconstructions derived from WA-PLS and RF were tested with the *randomTF* function of the *palaeoSig* package (Telford and Birks, 2011; Telford, 2013) in R.

In quantitative climate reconstructions, the taxonomic distance between a fossil pollen assemblage and its modern analogue is a key variable in evaluating the analogue quality (Birks et al., 1990). Shorter distances indicate closer taxonomic similarity and higher analogue quality, enhancing reconstruction reliability. This distance is commonly calculated using the squared chord distances based on the percentages of all pollen taxa. To evaluate the analogue quality, we calculated the squared chord distances between the selected fossil pollen spectra since the last glacial maximum (n=65, elevation higher than 3000 m a.s.l.; Cao et al., 2013) and the combined modern pollen dataset on the TP. The square chord distances were calculated using the *MAT* function of the *rioja* package (Juggins, 2018) in R.

https://doi.org/10.5194/essd-2025-242
Preprint. Discussion started: 10 July 2025

4 Data description

The pollen assemblages of the new surface-sediment samples (*n*=90) are dominated by herbaceous pollen from alpine meadow, steppe, and desert sites on the TP. In contrast, arboreal pollen dominates the samples collected from forest, consisting mainly of *Pinus*, *Picea*, *Alnus*, *Tsuga*, *Juniperus*, *Betula*, and *Quercus* (Fig. 2). Additionally, there are evident regional peculiarities in its distribution (Fig. 2–4). Sites with Cyperaceae abundances >60% from alpine meadows are more common than other sites, whereas steppe regions are marked by higher percentages of Poaceae and *Artemisia*, typically exceeding 30% and 50, respectively. The distribution center of Amaranthaceae (> 30%) is generally located in desert (Fig. 2–4; Table 2).

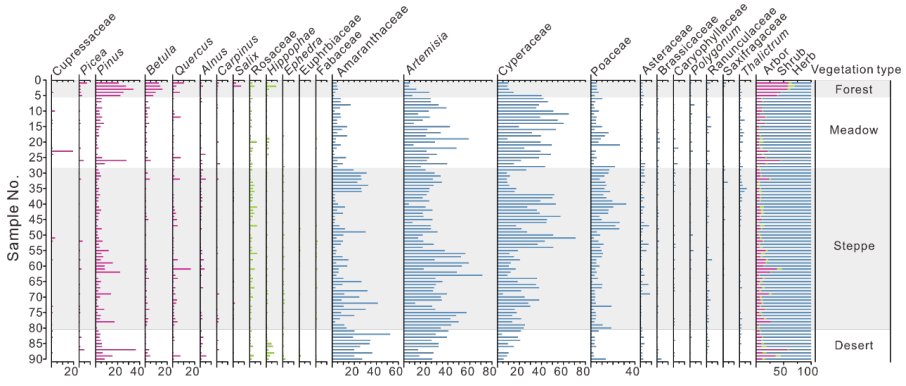

Figure 2. Percentage diagram of major pollen taxa for 90 lake surface-sediment samples on the Tibetan Plateau. Samples are arranged according to their vegetation type.

Group 1 (forest, *n*=5): The pollen assemblages of the sampled lakes are characterized by the lowest *Artemisia* and Amaranthaceae content, yet exhibits the highest arboreal pollen (AP) percentages among the four groups. Key arboreal taxa include *Pinus* (mean 26.0%, maximum 34.2%), *Betula* (mean 11.7%, maximum 15.6%), *Quercus* (mean 3.9%, maximum 9.3%), and *Picea* (mean 2.7%, maximum 7.0%, Fig. 2–4).

Group 2 (meadow, *n*=22): This group is typically characterized by the lowest AP and A/Cy (*Artemisia*/Cyperaceae) ratio but the highest Cyperaceae abundance (mean 39.8%, maximum 64.7%), with common taxa comprising *Artemesia* (mean 27.1%, maximum 58.9%), Amaranthaceae (mean 6.8%, maximum 16.4%), and Poaceae (mean 6.3%, maximum 26.1%, Fig. 2–4).

Group 3 (steppe, *n*=53): *Artemesia* (mean 28.9%, maximum 59.0%) is the most dominant component compared to meadow sites (Fig. 2–4). In addition, as a common taxon, Poaceae (mean 10.3%, maximum 31.4%), as well as the A/C (*Artemisia*/ Amaranthaceae (=Chenopodiaceae)) ratio (range 0.25–12.14, median 3.45) reach their highest values of the different vegetation types.

https://doi.org/10.5194/essd-2025-242
Preprint. Discussion started: 10 July 2025

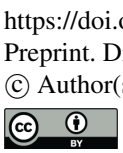

Open Access Earth System Science Data Discussions

Group 4 (desert, *n*=10): These sites are characterized by the highest percentages of Amaranthaceae (mean 26.7%, maximum 52.4%), with higher *Artemisia* abundance (mean 27.4%, maximum 40.2%, Fig. 2–4), and the lowest Poaceae (mean 3.1%, maximum 6.6%), Cyperaceae (mean 11.4%, maximum 21.1%), and A/C ratio (range 0.55–2.08, median 0.83).

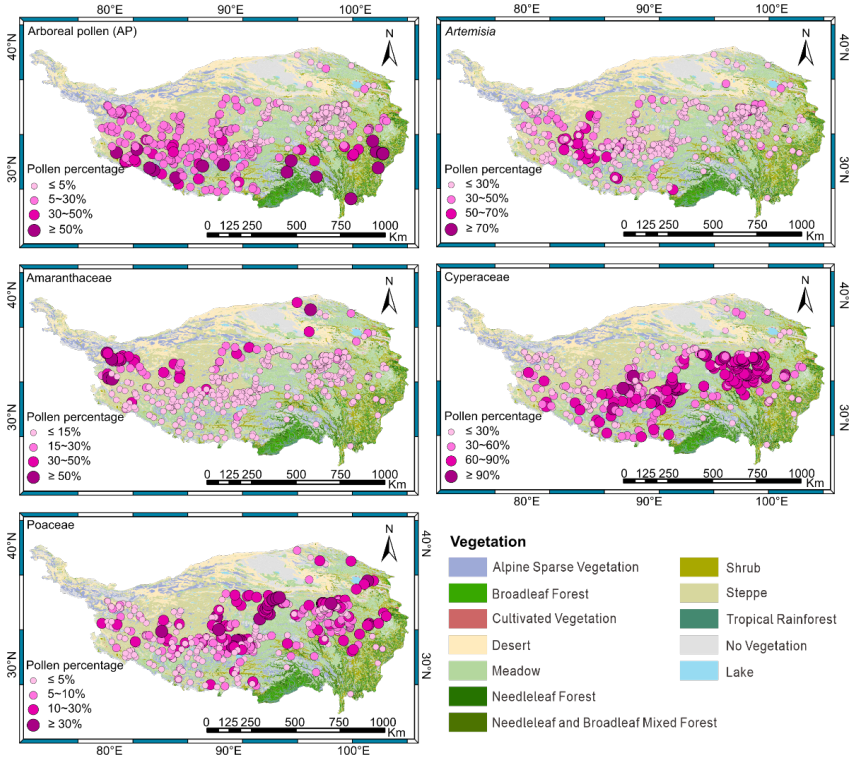

Figure 3. The spatial distribution maps of pollen percentages for total arboreal pollen (AP) and selected taxa (*Artemisia*, Amaranthaceae, Cyperaceae, Poaceae) in the dataset of lake surface-sediment samples (*n*=476) on the Tibetan Plateau.

Although AP pollen is detected at most meadow and steppe sites, and occasionally in desert regions, its abundance is markedly lower than in the forest sites (Table 1, Fig. 2–4). Since trees are absent in the alpine meadow, steppe, and desert communities on the TP (Wu, 1995; Wu and Xiao, 1995; Herzschuh et al., 2010), the low AP abundances likely represent wind-transported pollen transported from adjacent low-elevation regions. Despite this influence, the pollen assemblages effectively represent local vegetation composition, as the contribution of distant pollen is minimal overall (Fig. 2–4). Thus, the modern pollen distribution aligns closely with established vegetation types, corroborating findings from previous studies (Shen et al., 2006; Herzschuh et al., 2010;

https://doi.org/10.5194/essd-2025-242
Preprint. Discussion started: 10 July 2025

Li et al., 2020). Pollen assemblages of the 476 pollen samples of the dataset from TP are shown in Figure S1.

Table 2. Summary statistics of geophysical, climate variables, net primary production (NPP), and pollen percentages of the dataset on the Tibetan Plateau (*n*=476, Min: minimum; Med: median; Max: maximum, SD: standard deviation).

Parameter	Min.	Med.	Max.	SD.	Pollen taxa	Min.	Med.	Max.	SD.
Longlitude	79.36	91.76	102.55	91.88	Ericaceae	0.00	0.00	3.08	0.07
Latitude	27.62	33.13	39.36	32.93	Euphorbiaceae	0.00	0.00	30.94	0.23
Elevation	2668	4544	5433	4518	Fabaceae	0.00	0.20	5.53	0.40
Mt_{co}	-23.48	-14.33	-2.65	-14.15	Gentianaceae	0.00	0.00	6.49	0.25
Mt_{wa}	1.77	7.86	19.26	8.17	*Hippophae*	0.00	0.18	10.80	0.50
T_{ann}	-9.09	-2.71	6.93	-2.54	Lamiaceae	0.00	0.00	8.77	0.20
P_{ann}	97	351	788	390	*Picea*	0.00	0.18	10.63	0.51
NPP	0.16	444.70	6617.36	660.54	*Pinus*	0.00	1.60	64.98	5.80
Pollen taxa	Min.	Med.	Max.	SD.	Poaceae	0.00	5.32	87.74	9.51
Abies	0.00	0.00	8.59	0.23	Polemoniaceae	0.00	0.00	15.21	0.09
Alnus	0.00	0.17	8.86	0.48	*Polygonum*	0.00	0.23	20.50	0.69
Artemisia	0.00	11.3	70.05	16.28	*Quercus*_deciduous	0.00	0.00	5.21	0.07
Asteraceae	0.00	1.70	33.56	16.28	*Quercus*_evergreen	0.00	0.00	27.81	1.17
Betula	0.00	0.36	30.59	1.49	Ranunculaceae	0.00	1.00	84.46	0.01
Brassicaceae	0.00	0.37	28.17	0.96	*Rheum*	0.00	0.00	3.73	2.53
Caryophyllaceae	0.00	0.30	10.79	0.59	Rosaceae	0.00	1.00	17.41	0.30
Amaranthaceae	0.00	2.08	64.89	6.54	*Salix*	0.00	0.00	7.16	1.76
Crassulaceae	0.00	0.00	2.49	0.06	*Thalictrum*	0.00	0.63	12.05	0.33
Cupressaceae	0.00	0.00	88.50	0.83	Saxifragaceae	0.00	0.00	4.69	1.10
Cyperaceae	0.00	38.37	96.68	43.01	Thymelaeaceae	0.00	0.00	8.33	0.12
Ephedra	0.00	0.15	7.45	0.36	*Tsuga*	0.00	0.00	6.47	0.03
Ericaceae	0.00	0.00	3.08	0.07	*Urtica*	0.00	0.00	3.87	0.23

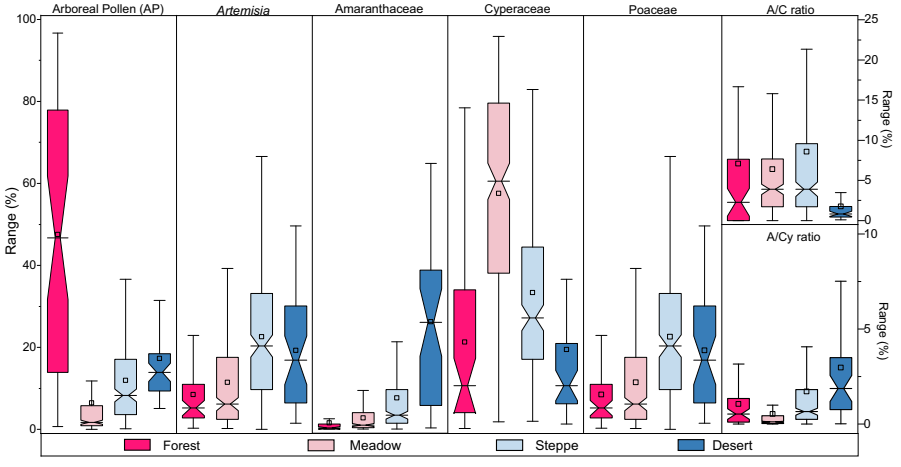

https://doi.org/10.5194/essd-2025-242
Preprint. Discussion started: 10 July 2025

Figure 4. Box plots of the regional percentage distributions of arboreal pollen (AP) and four selected pollen types (*Artemisia*, Amaranthaceae, Cyperaceae, Poaceae), plus the ratios of A/C (*Artemisia*/Amaranthaceae (=Chenopodiaceae)) and A/Cy (*Artemisia*/Cyperaceae) from modern lake surface-sediment samples across the Tibetan Plateau.

The initial RDA indicated variance inflation factor (VIF) values exceeding 20 for the variables T_{ann}, Mt_{co}, and Mt_{wa}. However, after deleting T_{ann}, which had the highest VIF value, the remaining four variables (P_{ann}, Mt_{co}, Mt_{wa}, and NPP) had VIF values lower than 20. Thus, they are used in the final RDA to discern their influence on the modern pollen dataset.

Table 3. Summary statistics of redundancy analysis (RDA) of 476 sites, 35 pollen types, and four climatic variables (P_{ann}: mean annual precipitation, mm; Mt_{co}: mean temperature of the coldest month, °C; Mt_{wa}: mean temperature of the warmest month, °C; T_{ann}: annual mean temperature, °C) and NPP (net primary production) in the pollen dataset from the Tibetan Plateau. VIF: variance inflation factor.

Climatic variables	VIF (without T_{ann})	VIF (with T_{ann})	λ_1/λ_2	Climatic variables as sole predictor	Marginal contribution based on climatic variables	
				Explained variance (%)	Explained variance (%)	P-value
NPP	1.94	2.19	0.21	7.29	0.67	0.006
P_{ann}	3.10	3.43	0.44	13.13	3.92	0.001
Mt_{co}	2.84	80.97	0.09	3.37	2.70	0.001
Mt_{wa}	2.90	41.11	0.15	5.04	1.03	0.001
T_{ann}	—	185.28	—	—	—	—

The RDA results highlight that, as a sole predictor, relative to Mt_{co} and Mt_{wa}, P_{ann} and NPP explain ubstantial portions of pollen assemblage variation (13.13% and 6.97%, respectively) in the dataset (Table 3). A biplot of the RDA shows that the vectors for both P_{ann} and NPP form smaller angles with the positive direction of axis 1 (capturing 34.7% of total inertia in the dataset) compare to axis 2 (15.7%), suggesting moisture availability as the primary determinant along axis 1 (Fig. 5). RDA axis 1, which is highly correlated with NPP and P_{ann}, generally divides the pollen taxa into two groups. One group, comprising Cyperaceae, Ranunculaceae, and *Salix*, indicates wet climatic conditions (located along the positive direction of P_{ann}), while the other group, consisting of *Artemisia*, Amaranthaceae, Poaceae, *Ephedra*, and Saxifragaceae represents drought (located along the negative direction of P_{ann}; Fig. 5).

https://doi.org/10.5194/essd-2025-242
Preprint. Discussion started: 10 July 2025

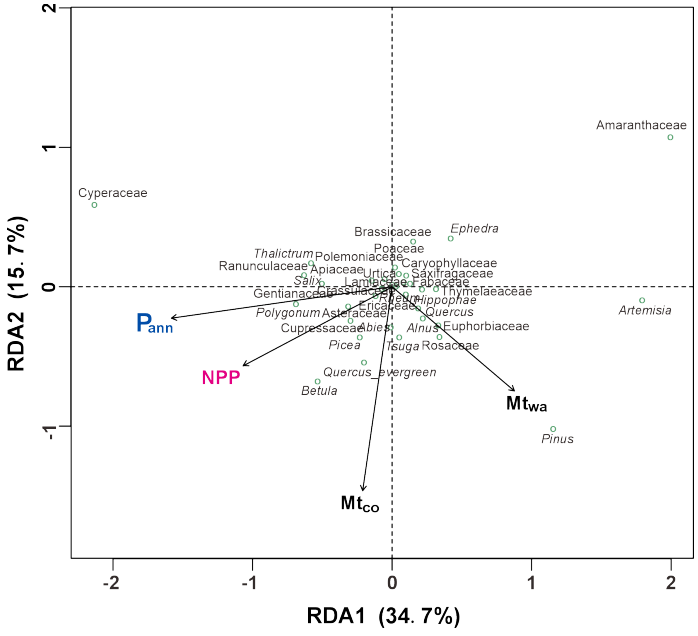

Figure 5. Redundancy analysis (RDA) biplot of the pollen dataset based on the first two axes showing the relationships between 35 pollen taxa (circles) and four variables (arrows) (P_{ann}: mean annual precipitation, mm; Mt_{co}: mean temperature of the coldest month, °C; Mt_{wa}: mean temperature of the warmest month, °C, and NPP: net primary production, Kg C m^{-2}).

5 Potential use of the lake surface-sediment pollen dataset

In the calibration-sets, P_{ann} and NPP are selected as the target variables, as their identified importance in influencing pollen distribution, with NPP further providing insights into alpine vegetation conditions. The pollen-based modern P_{ann} and NPP estimations using both WA-PLS and RF approaches match original measurements well, with a high coefficient of determination between observed and predicted variables (R^2) and low root mean square error of prediction (RMSEP) (Fig. 6). the RF model showed superior predictive performance compared to WA-PLS for both target variables.

Reconstructions covering P_{ann} of ca. 300–600 mm and NPP lower than 1000 Kg C m^{-2} should be reliable because their bias is low (Fig. 6). For P_{ann}, the proportion of residuals between -50 and 50 mm derived from RF (48.1%) is slightly higher than that of WA-PLS (45.6%). Similarly, for the range of -100 to 100 mm, RF (71.8%) outperforms WA-PLS (65.8%). For NPP, RF also shows a notably higher proportion of residuals between -500 and 500 Kg C m^{-2} (84.5%) compared to WA-PLS (74.8%). This advantage persists for the narrower range of -300 to 300 kg C m^{-2} (RF: 63.9% vs. WA-PLS: 50.4%). However, both models consistently overestimated Pann and NPP in arid areas with low productivity and underestimated these variables in humid, high-

https://doi.org/10.5194/essd-2025-242
Preprint. Discussion started: 10 July 2025

315 productivity areas, highlighting the necessity of addressing the "edge-effect" (Fig. 6, 7).
316

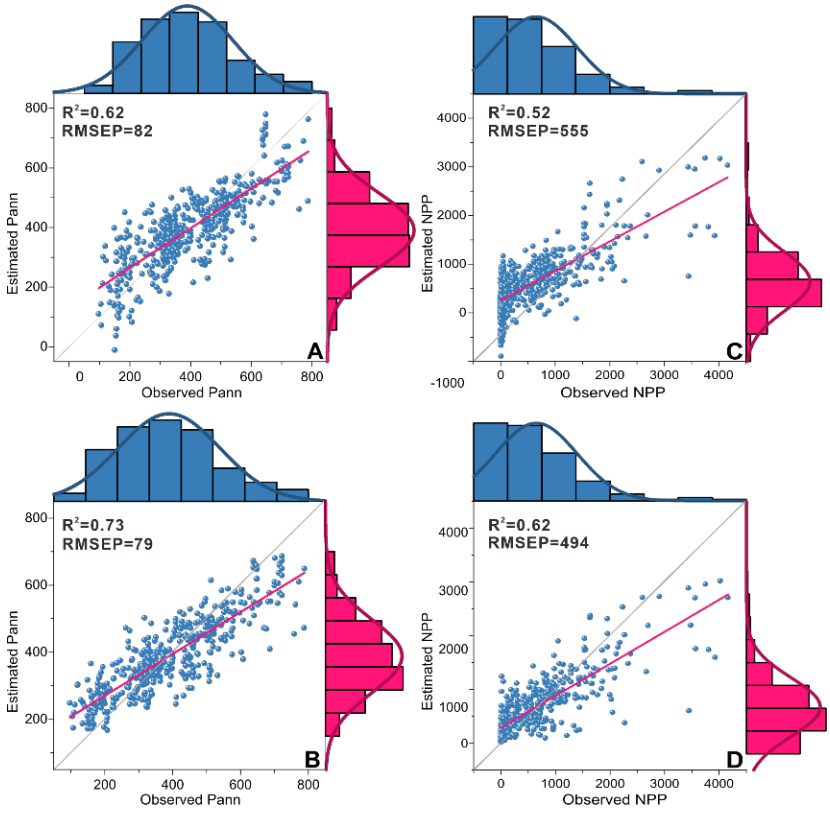

317
318 **Figure 6**. Scatter plots of observed mean annual precipitation (P_{ann}) vs. predicted P_{ann}, observed net
319 primary production (NPP) vs. predicted NPP using weighted-averaging partial least squares
320 regression (WA-PLS: top row) and random forest (RF: bottom row) based on the pollen data (n=476)
321 from lake surface-sediments on the Tibetan Plateau (R^2: coefficient of determination between
322 observed and predicted values; RMSEP: root mean square error of prediction produced by "leave-
323 one-out" cross-validation).

https://doi.org/10.5194/essd-2025-242
Preprint. Discussion started: 10 July 2025

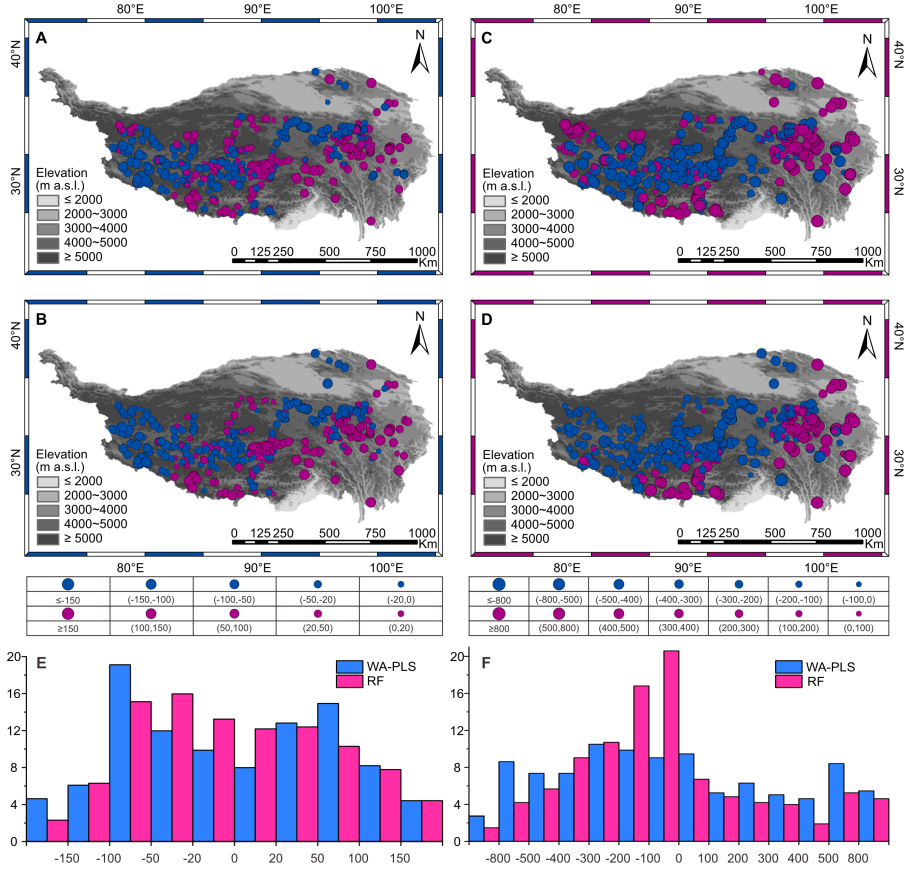

Figure 7. The residuals between observations and pollen-based reconstructions for the lake surface-sediment sites (n=476) on the Tibetan Plateau: (A) mean annual precipitation (P_{ann}) by weighted-averaging partial least squares regression (WA-PLS) and (B) random forest (RF), (C) net primary production (NPP) by WA-PLS and (D) RF. The two bar charts in the lower part of the figure show the proportions of modern pollen sites available within different ranges of residuals (observation minus reconstruction) for both P_{ann} (E) and NPP (F).

Most of the poor analogue assemblages come from the TP margin and date back to >12 cal ka BP, which is possibly related to the higher abundance of arboreal pollen in this specific period and region (Fig. 8). While our combined modern pollen dataset from lake surface-sediments can provide good analogues for fossil pollen assemblages and enhance the performance of palaeoclimate reconstructions on the central TP, caution remains warranted for interpreting pollen assemblages from plateau margins and periods earlier than the Holocene (Fig. 8).

https://doi.org/10.5194/essd-2025-242
Preprint. Discussion started: 10 July 2025

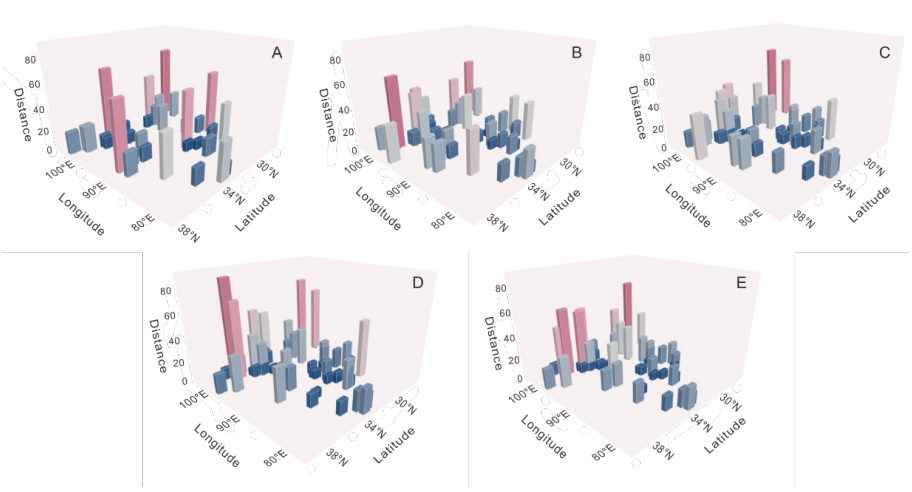

Figure 8. Spatial distribution of analogue quality for six key time slices on the Tibetan Plateau: (A) 15–12 cal ka BP; (B) 12–9 cal ka BP; (C) 9–6 cal ka BP; (D) 6–3 cal ka BP; (E) 3–0 cal ka BP.

6 Data availability

The modern pollen dataset from lake surface-sediment samples (n=90) comprising pollen percentages, site locations, net primary production, and climatic data for each lake is accessible from the National Tibetan Plateau / Third Pole Environment Data Center (TPDC; Tian, 2025; https://doi.org/10.11888/Paleoenv.tpdc.302470).

7 Summary

We established a comprehensive modern pollen dataset extracted from lake surface-sediments in forest, meadow, steppe, and desert vegetation types on the Tibetan Plateau by combining new modern pollen data with previous datasets. Numerical analyses reveal that mean annual precipitation (P_{ann}) is the most important climatic determinant influencing pollen distribution. Our dataset has good predictive power for past net primary production (NPP) and P_{ann} reconstructions. The random forest algorithm is found to be a reliable approach for pollen-based reconstructions of past environments.

The pollen data from our sampled lakes help to fill the geographical gap left by previously published modern pollen datasets, thereby improving the spatial distribution of sampling sites covering the Tibetan Plateau. Our dataset is a key component for providing quantitative estimates of past vegetation or climate, and can also be integrated with other pollen datasets in the future to improve the reliability of past ecosystem and climate reconstructions on the Tibetan Plateau.

Author contributions. FT designed the pollen dataset, FT, WC, XC collected the samples, WC performed pollen extraction and identification. XC and FT compiled the

https://doi.org/10.5194/essd-2025-242
Preprint. Discussion started: 10 July 2025

standardization for the dataset, performed numerical analyses, and organized the manuscript. WC prepared the figures and tables. All authors discussed the results and contributed to the final paper.

Competing interests. The corresponding author declares that none of the authors has any competing interests.

Disclaimer. Publisher's note: Copernicus Publications remains neutral with regard to jurisdictional claims in published maps and institutional affiliations.

Acknowledgements. The authors would like to express their gratitude to the palynologists Ulrike Herzschuh (Alfred Wegener Institute Helmholtz Center for Polar and Marine Research), Chunhai Li (Nanjing Institute of Geography and Limnology, Chinese Academy of Sciences), Kai Li (College of Life Sciences, Zhejiang Normal University), Qingfeng Ma (Institute of Tibetan Plateau Research, Chinese Academy of Sciences) who contributed to the dataset. We thank Zhitong Chen (Institute of Tibetan Plateau Research, Chinese Academy of Sciences), and students Meijiao Chen, Yunqing Li, and Anjing Jian for their help with sample collections in the field work, and Cathy Jenks with the help of language editing.

Financial support. This research was supported by the National Natural Science Foundation of China (Grant No. 42471179, 42071107).

References

Birks, H. J. B. (Eds.): Quantitative palaeoenvironmental reconstructions. Statistical modelling of Quaternary science data, Vol. 5, Technical guide (ed. by D. Maddy and J.S. Brew), Quaternary Research Association, Cambridge, UK, 271 pp., https://w2.uib.no/filearchive/95birks_qpr_in_maddybrew_1.pdf, 1995.

Birks, H. J. B.: Numerical tools in palaeolimnology–Progress, potentialities, and problems, J. Paleolimnol., 20, 307–332, https://doi.org/10.1023/A:1008038808690, 1998.

Birks, H. J. B., Line, J. M., Juggins, S., Stevenson, A. C., and ter Braak, C. J. F.: Diatoms and pH reconstruction, Philos. T. R. Soc. B, 327, 263–278, https://doi. org/10.1098/rstb.1990.0062, 1990.

ter Braak, C. J. F., and Juggins S.: Weighted averaging partial least squares regression (WA-PLS): an improved method for reconstructing environmental variables from species assemblages, Hydrobiologia, 269, 485–502, https://doi.org/10.1007/BF00028046, 1993.

ter Braak, C. J. F., and Prentice, I. C.: A theory of gradient analysis, Adv. Ecol. Res., 18, 271–317, https://doi.org/10.1016/S0065-2504(03)34003-6, 1988.

ter Braak, C. J. F., and Verdonschot, P. F. M.: Canonical correspondence analysis and related multivariate methods in aquatic ecology, Aquat. Sci., 57, 255–289, https://doi.org/10.1007/BF00877430, 1995.

https://doi.org/10.5194/essd-2025-242
Preprint. Discussion started: 10 July 2025

403 Breiman, L.: Random Forests, Mach. Learn, 45, 5–32, https://doi.org/10.1023/A:1010933404324,
404 2001.
405 Cao, X., Herzschuh, U., Telford, R. J., and Ni, J.: A modern pollen–climate dataset from China and
406 Mongolia: Assessing its potential for climate reconstruction, Rev. Palaeobot. Palynol., 211, 87–
407 96, https://doi.org/10.1016/j.revpalbo.2014.08.007, 2014.
408 Cao, X., Ni, J., Herzschuh, U., Wang, Y., and Zhao, Y.: A late Quaternary pollen dataset from eastern
409 continental Asia for vegetation and climate reconstructions: Set up and evaluation, Rev. Palaeobot.
410 Palynol., 194, 21–37, https://doi.org/10.1016/j.revpalbo.2013.02.003, 2013.
411 Cao, X., Tian, F., Andreev, A., Anderson, P. M., Lozhkin, A. V., Bezrukova, E., Ni, J., Rudaya, N.,
412 Stobbe, A., Wieczorek, M., and Herzschuh, U.: A taxonomically harmonized and temporally
413 standardized fossil pollen dataset from Siberia covering the last 40 kyr, Earth Syst. Sci. Data, 12,
414 119–135, https://doi.org/10.5194/essd-12-119-2020, 2020.
415 Cao, X., Tian, F., Li, K., Ni, J., Yu, X., Liu, L., and Wang, N.: Lake surface sediment pollen dataset
416 for the alpine meadow vegetation type from the eastern Tibetan Plateau and its potential in past
417 climate reconstructions, Earth Syst. Sci. Data, 12, 119–135, 13, 3525–3537,
418 https://doi.org/10.5194/essd-13-3525-2021, 2021.
419 Chen, F., Dong, G., Zhang, D., Liu, X., Jia, X., An, C., Ma, M., Xie, Y., Barton, L., Ren, X., Zhao,
420 Z., Wu, X., and Jones, M. K.: Agriculture facilitated permanent human occupation of the Tibetan
421 Plateau after 3600 B.P., Science, 347, 248–250, https://doi.org/10.1126/science.aaa7573, 2015.
422 Chen, F., Zhang, J., Liu, J., Cao, X., Hou, J., Zhu, L., Xu, X., Liu, X., Wang, M., Wu, D., Huang, L.,
423 Zeng, T., Zhang, S., Huang, W., Zhang, X., and Yang, K.: Climate change, vegetation history, and
424 landscape responses on the Tibetan Plateau during the Holocene: a comprehensive review, Quat.
425 Sci. Rev., https://doi.org/10.1016/j.quascirev.2020.106444 243, 106444, 2020.
426 Fægri, K., and Iversen, J. (Eds.): Text book of pollen analysis (4th Edition), John Wiley and Sons
427 Press, Chichester, UK, 328 pp., https://doi.org/10.1002/jqs.3390050310, 1989.
428 Fang, J., Piao, S., Tang, Z., Peng, C., and Ji, W.: Interannual variability in net primary production
429 and precipitation, Science, 293, 1723. https://doi.org/10.1126/ science.293.5536.1723a, 2001.
430 Gonsamo, A., Chen, J., Price, D. T., Kurz, W. A., Liu, J., Boisvenue, C., Hember, R. A., Wu, C., and
431 Chang, K.: Improved assessment of gross and net primary productivity of Canada's landmass, J.
432 Geophys. Res. Biogeosci., 118, 1546–1560, https://doi.org/10.1002/2013JG002388, 2013.
433 Grimm, E. C.: CONISS: A FORTRAN 77 program for stratigraphically constrained cluster analysis
434 by the method of incremental sum of squares, Comput. Geosci., 13, 13–35,
435 https://doi.org/10.1016/0098-3004(87)90022-7, 1987.
436 Grimm, E. C.: Tilia and Tilia-Graph Software. Springfield, IL: Illinois State Museum [code],
437 https://www.neotomadb.org/apps/tilia, 1991.
438 He, J., Yang, K., Tang, W., Lu, H., Qin, J., Chen, Y., and Li, X.: The first high-resolution
439 meteorological forcing dataset for land process studies over China, Sci. Data, 7, 25,
440 https://doi.org/10.1038/s41597-020-0369-y, 2020.
441 Herzschuh, U.: Reliability of pollen ratios for environmental reconstructions on the Tibetan Plateau,
442 J. Biogeogr., 34, 1265–1273, https://doi.org/10.1111/j.1365-2699.2006.01680.x, 2007.
443 Herzschuh, U., Birks, H. J. B., Mischke, S., Zhang, C., and Böhner, J.: A modern pollen-climate
444 calibration set based on lake sediments from the Tibetan Plateau and its application to a Late
445 Quaternary pollen record from the Qilian Mountains, J. Biogeogr., 37, 752–766,
446 https://doi.org/10.1111/j.1365-2699.2009.02245.x, 2010.

https://doi.org/10.5194/essd-2025-242
Preprint. Discussion started: 10 July 2025

Hill, M. O., and Gauch, H. G.: Detrended correspondence analysis: an improved ordination technique, Vegetatio, 42, 41–58, https://doi.org/10.1007/BF00048870, 1980.

Ji, Y., Zhou, G., Luo, T., Dan, Y., Zhou, L., and Lu, X.: Variation of net primary productivity and its drivers in China's forests during 2000–2018, Forest Ecosystems 7:15, https://doi.org/10.1186/s40663-020-00229-0, 2020.

Jin, Y., Zhou, K., Gao, J., Mu, S., and Zhang, X.: Identifying the priority conservation areas for key national protected terrestrial vertebrate species based on a random forest model in China, Aeta Ecol. Sin. 36 (23), 7702–7712, 2016. (in Chinese)

Juggins, S.: rioja: Analysis of Quaternary Science Data. version 0.7–3. Juggins, S. [code], https://doi.org/10.32614/CRAN.package.rioja, 2012.

Juggins, S.: Quantitative reconstructions in palaeolimnology: new paradigm or sick science? Quat. Sci. Rev., 64, 20–32, https://doi.org/10.1016/j.quascirev.2012.12.014, 2013.

Juggins, S.: rioja: Analysis of quaternary science data, version 0.9–15.1. Juggins, S. [code], https://doi.org/10.32614/CRAN.package.rioja, 2018.

Juggins, S., and Birks, H. J. B.: Quantitative Environmental Reconstructions from Biological Data. In: Birks, H. J. B., Lotter, A. F., Juggins, S., Smol, J. P. (Eds.), Tracking Environmental Change Using Lake Sediments, Vol. 5: Data Handling and Numerical Techniques, Springer, Dordrecht, Netherlands, 64 pp., https://doi.org/10.1007/978-94-007-2745-8_14, 2012.

Li, C., and Li, Y.: Study of modern pollen and stomata from surficial lacustrine sediments from the eastern edge of Tibetan Plateau, China, Rev. Palaeobot. Palynol., 221, 184–191, https://doi.org/10.1016/j.revpalbo.2015.07.006, 2015.

Li, J., Xie, G., Yang, J., Ferguson, D. F., Liu, X., Liu, H., and Wang, Y. F.: Asian Summer Monsoon changes the pollen flow on the Tibetan Plateau, Earth Sci. Rev., 202, 103114, https://doi.org/10.1016/j.earscirev.2020.103114, 2020.

Li, X.: Using "random forest" for classification and regression, Chinese J. Appl. Entomol. 50, 1190–1197, 2013. (in Chinese)

Liaw, A.: Random Forest: Breiman and Cutler's Random Forests for Classification and Regression, version 4.6–14, available at: https://cran.r-project.org/web/packages/randomForest/index.html, 2018.

Ma, Q., Zhu, L., Ju, J., Wang, J., Wang, Y., Huang, L., and Haberzettl, T.: A modern pollen dataset from lake surface sediments on the central and western Tibetan Plateau, Earth Syst. Sci. Data, 16, 311–320, https://doi.org/10.5194/essd-16-311-2024, 2024.

Ma, Q., Zhu, L., Wang, J., Ju, J., Lü, X., Wang, Y., Guo, Y., Yang, R., Kasper, T., Haberzettl, T., and Tang, L.: Artemisia/Chenopodiaceae ratio from surface lake sediments on the central and western Tibetan Plateau and its application, Palaeogeogr. Palaeocl., 479, 138–145, https://doi.org/10.1016/j.palaeo.2017.05.002, 2017.

Maher, L. J.: Statistics for microfossil concentration measurements employing samples spiked with marker grains, Rev. Palaeobot. Palynol., 32 (2–3), 153–191, https://doi.org/10.1016/0034-6667(81)90002-6, 1981.

Nemani, R. R., Keeling, C. D., Hashimoto, H., Jolly, W. M., Piper, S. C., Tucker, C. J., Myneni, R. B., and Running, S. W.: Climate-driven increases in global terrestrial net primary production from 1982 to 1999, Science, 300, 1560–1563, https://doi.org/10.1126/science.1082750, 2003.

Ni, J.: Carbon storage in Chinese terrestrial ecosystems: approaching a more accurate estimate, Clim. Change, 119, 905–917, https://doi.org/10.1007/s10584-013-0767-7, 2013.

https://doi.org/10.5194/essd-2025-242
Preprint. Discussion started: 10 July 2025

491 Nychka, D., Furrer, R., Paige, J., and Sain, S.: fields: Tools for spatial data, version 16.3.1 [code],
492 https://doi.org/10.32614/CRAN.package.fields, 2025.
493 Oksanen, J, Blanchet, F. G., Friendly, M., Kindt, R., Legendre, P., McGlinn, D., Minchin, P. R.,
494 O'Hara, R. B., Simpson, G. L., Solymos, P., Stevens, M. H. H., Szoecs, E., and Wagner, H.: vegan:
495 Community Ecology Package, version 2.0–4 [code], https://cran.r-project.org/web/packages/ve-
496 gan/index.html, 2019.
497 Pepin, N., Bradley, R. S., Diaz, H. F., Baraer, M., Caceres, E. B., Forsythe, N., Fowler, H.,
498 Greenwood, G., Hashmi, M. Z., and Liu, X. D.: Elevation-dependent warming in mountain
499 regions of the world, Nature Clim. Change, https://doi.org/10.1038/nclimate2563, 2015.
500 Prentice, I. C.: Multidimensional scaling as a research tool in Quaternary palynology: a review of
501 theory and methods, Rev. Palaeobot. Palynol., 31, 71–104, https://doi.org/10.1016/0034-
502 6667(80)90023-8, 1980.
503 Qin F.: Modern pollen assemblages of the surface lake sediments from the steppe and desert zones
504 of the Tibetan Plateau, Sci. China Earth Sci., 64, 425–439, https://doi.org/10.1007/s11430-020-
505 9693-y, 2021.
506 Qin, F., Zhao, Y., and Cao, X.: Biome reconstruction on the Tibetan Plateau since the Last Glacial
507 Maximum using a machine learning method, Sci. China Earth Sci., 65, 518–535,
508 https://doi.org/10.1007/s11430-021-9867-1, 2022.
509 R Core Team: R, A language and environment for statistical computing, R Foundation for Statistical
510 Computing [code], https://www.r-project.org, 2019.
511 Shen, C., Liu, K., Tang, L., and Overpeck, J. T.: Quantitative relationships between modern pollen
512 rain and climate in the Tibetan Plateau, Rev. Palaeobot. Palynol., 140, 61–77,
513 https://doi.org/10.1016/j.revpalbo.2006.03.001, 2006.
514 Sun, H. (Eds.): The national physical atlas of China, China Cartographic Publishing House, Beijing,
515 China, 283 pp., ISBN 9787503120398, 1999.
516 Tang, L., Mao, L., Shu, J., Li, C., Shen, C., and Zhou, Z. (Eds.): An Illustrated Handbook of
517 Quaternary Pollen and Spores in China, Science Press, Beijing, China, 620 pp.,
518 ISBN9787030505682, 2016. (in Chinese)
519 Telford, R. J., and Birks, H. J. B.: Effect of uneven sampling along an environmental gradient on
520 transfer-function performance, J. Paleolimnol., 46, 99–106, https://doi.org/10.1007/s10933-011-
521 9523-z, 2011.
522 Telford, R. J.: palaeoSig: significance tests for palaeoenvironmental reconstructions, version 1.1–2,
523 Telford, R. J. [code], https://doi.org/10.32614/CRAN.package.palaeoSig, 2013.
524 Tian, F., Cao, X., Zhang, R., Xu, Q., Ding, W., Liu, X., Pan, B., and Chen, J.: Spatial homogenization
525 of soil-surface pollen assemblages improves the reliability of pollen-climate calibration-set, Sci.
526 China Earth Sci., 63, 1758–1766, https://doi.org/10.1007/s11430-019-9643-0, 2020.
527 Tian, F., Cao, W., Liu, X., Liu, Z., and Cao, X.: Pollen assemblages of lake surface sediment across
528 the Tibetan Plateau, National Tibetan Plateau / Third Pole Environment Data Center [data set],
529 https://doi.org/10.11888/Paleoenv.tpdc.302470, 2025.
530 Tian, F., Wang, W., Rudaya, N., Liu, X., and Cao, X.: Wet mid–late Holocene in central Asia
531 supported prehistoric intercontinental cultural communication: Clues from pollen data, Catena,
532 209, 105852, https://doi.org/10.1016/j.catena.2021.105852, 2022.
533 Walker, A. P., Zaehle, S., Medlyn, B. E., De Kauwe, M. G., Asao, S., Hickler, T., Parton, W., Ricciuto,
534 D. M., Wang, Y., Wårlind, D., and Norby, R. J.: Predicting long-term carbon sequestration in

https://doi.org/10.5194/essd-2025-242
Preprint. Discussion started: 10 July 2025

response to CO_2 enrichment: how and why do current ecosystem models differ? Global Biogeochem. Cycles, 29, 476–495, https://doi.org/10.1002/2014GB004995, 2015.

Wang, B. (Eds.): The Asian Monsoon, Springer, Chichester, UK, 845 pp., https://doi.org/10.1007/3-540-37722-0, 2006.

Wang, F., Qian, N., Zhang, Y., and Yang, H. (Eds.): Pollen Flora of China, 2nd Edition, Science Press, Beijing, China, 461 pp., ISBN7030036352, 1995. (in Chinese)

Wu, K., Li, K., Jia, W., Stoof-Leichsenring, K. R., Herzschuh, U., Ni, J., Liao, M., and Tian, F.: Application of plant DNA metabarcoding of lake sediments for monitoring vegetation compositions on the Tibetan Plateau, Sci. China Earth Sci., 67, 3594–3609, https://doi.org/10.1007/s11430-023-1358-0, 2024.

Wu, Y., and Xiao, J.: A preliminary study on modern pollen rain of Zabuye Salt Lake area, Xizang, Plant Divers., 17, 72–78, https://journal.kib.ac.cn/EN/Y1995/V17/I01/1, 1995. (in Chinese)

Wu, Z. (Eds.): The vegetation of China, Science Press, Beijing, China, 1270 pp., ISBN 7030024222, 1995. (in Chinese)

Yue, P., Lu, X., Ye, R., Zhang, C., Yang, S., Zhou, Y., and Peng, M.: Distribution of Stipa purpurea steppe in the Northeastern Qinghai-Xizang Plateau (China), Russ. J. Ecol., 42, 50–56, https://doi.org/10.1134/S1067413611010140, 2011.

Zhang, X.: Vegetation Map of China and Its Geographic Pattern-Illustration of the Vegetation Map of the People's Republic of China (1:1000000), Geology Press, Beijing, China, https://doi.org/10.12282/plantdata.0155, 2007. (in Chinese)

Zhao, M., and Running, S. W.: Drought-Induced Reduction in Global Terrestrial Net Primary Production from 2000 Through 2009, Science, 329, 940–943, https://doi.org/10.1126/science.1192666, 2010.